Int. J. Heat Mass Transfer. Vol. 5, pp. 469–487. Pergamon Press 1962. Printed in Great Britain.

AN ANALYTICAL AND EXPERIMENTAL STUDY OF TURBULENT GAS FLOW BETWEEN TWO SMOOTH PARALLEL WALLS WITH UNEQUAL HEAT FLUXES

H. BARROW

Department of Mechanical Engineering,
Walker & Harrison-Hughes Engineering Laboratories, The University of Liverpool, Liverpool

(*Received* 5 *October* 1961, *and in revised form* 7 *December* 1961)

Abstract—This paper contains the results of a theoretical and experimental study of asymmetric heat transfer to air in fully developed turbulent flow between two smooth parallel plates. The heat fluxes at the plate surfaces were of different magnitude; in the theoretical analysis, each surface heat flux was assumed to be uniform in the flow direction. In the experimental work, two-dimensional flow was simulated by means of long ducts of large aspect ratio.

Velocity distribution and friction data in adiabatic flow were recorded, and these showed good agreement with accepted relationships. Heat-transfer measurements were made firstly with one wall insulated and then with heat transfer at both walls. In the latter series of experiments, the wall fluxes were unequal and of opposite sign. The experimental heat-transfer coefficient for the wall through which heat was transferred to the fluid was observed to be less than the accepted value for the case of symmetrical heat transfer and to decrease as the degree of asymmetry increases. A decrease in heat transfer coefficient of up to about 40 per cent was measured.

The theory, which is based on the analogy between the transfers of heat and momentum, is more rigorous than that published by the author in a previous paper and is adequately supported by the experimental data.

It is concluded that the heat-transfer coefficient is dependent on the heat-flux distribution around the circumference of the flow section.

NOMENCLATURE

A,	cross-sectional area of duct;
A_s,	surface area
c,	specific heat at constant pressure;
C,	constant;
$De(=2s)$,	equivalent diameter, two-dimensional basis;
$D'_e(=4A/P)$,	equivalent diameter, channel basis;
e,	emissivity;
ϵ,	eddy diffusivity;
$f(=\tau_w/\frac{1}{2}\rho\bar{u}^2)$,	friction factor;
F,	function;
$G(=\bar{u}\rho)$,	mass velocity;
$h[=q_w/(T_w-T_B)]$	heat-transfer coefficient (bottom wall);
$I, I_1, I_2 \ldots,$	integrals;
κ,	thermal conductivity;
$\alpha(=\kappa/c\rho)$,	thermal diffusivity;
ρ,	density;
σ,	Stefan – Boltzmann constant;
p,	pressure;
P,	perimeter;
q,	heat flux;
s,	plate spacing;
T,	temperature;
τ,	shear stress;
$u, \bar{u}, u_\tau=\sqrt{(\tau_w/\rho)}, u_c$,	local, average, friction and centre-line velocities;
x,	distance in flow direction;
y,	wall distance;
$\mu, \nu(=\mu/\rho)$,	absolute and kinematic viscosities;

$u^+(=u/u_\tau)$, dimensionless velocity parameter;

$y^+\left(=\frac{yu_\tau}{\nu}\right)$, $s^+\left(=\frac{su_\tau}{\nu}\right)$, dimensionless distance parameters;

$Re(=2s\bar{u}/\nu)$, Reynolds number (two-dimensional);

$Re'(=(4A/P)\bar{u}/\nu)$, Reynolds number (channel);

$Nu(=hD_e/\kappa)$, Nusselt number;

$Pr(=c\mu/\kappa)$, Prandtl number.

Suffixes

B, bulk;
c, centre-line;
w, bottom wall;
o, upper wall;
a, environment (or ambient);
i, inlet;
s, surface;
M, momentum;
H, heat;
1, value at the outside of the laminar and transition region;
2, value at $y = s/3$.

1. INTRODUCTION

PIPE or tube flow with uniform heat transfer around the circumference has been the subject of many theoretical and experimental investigations. Many types of fluid have been examined and the whole range of flow pattern has been studied. Pipe flow is a convenient mechanical arrangement, but frequently the engineer finds it necessary to employ ducts whose shapes are not circular. A typical example of a non-circular flow section is the annular coolant passage around a nuclear fuel rod. The flow pattern in such sections is no longer a simple one, and sometimes the added complication of asymmetric heat transfer arises. The velocity and temperature fields perpendicular to the flow are dissimilar, and it is clear that the heat-flux distribution around the boundary of the flow is a variable of the problem.

The use of dimensional analysis for the solution of heat transfer in the case of the round pipe is well known, but when it is used in asymmetrical heat-transfer problems, care must be exercised. An observation on the use and limitations of this approach in non-uniform heat transfer has been made by the author [1]. The alternative method of solution which employs the analogy between the heat and momentum transfers is not directly applicable in asymmetric cases; an example of how the analogy may be modified is recorded in a previous analytical paper by the author [2]. This work [2] was a preliminary attempt to establish the dependence of heat transfer on heat-flux distribution around a non-circular flow section. The present paper may be considered as an extension of this earlier study and is concerned with fully developed turbulent flow between two smooth plates with unequal heat fluxes. Both wall heat fluxes are uniform in the flow direction. The idealized model is shown in Fig. 1. The degree of asymmetry is measured by

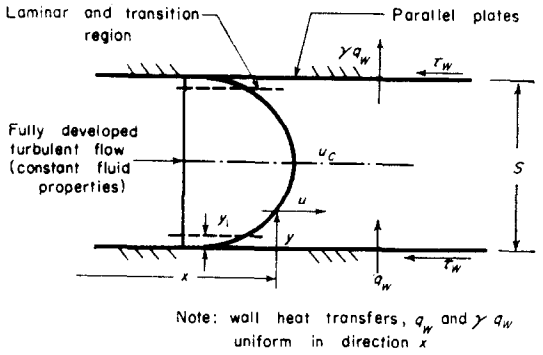

FIG. 1. Idealized model.

means of a parameter γ which can take either positive or negative values. The previous simple analysis [2] showed that the heat transfer coefficient is a function of γ, Re and Pr. The more rigorous theory of the present work is given in detail in Appendix A. Beginning with the fundamental equations of heat and momentum transfer, and using more realistic distributions of velocity and eddy diffusivity, we may predict the temperature and heat transfer.

In an effort to detect the effect of asymmetry on heat transfer, an experimental programme was devised and the results are reported here. The working fluid was air.

2. APPARATUS AND EXPERIMENTAL PROGRAMME

The experimental work was conducted in

three parts. In the first phase, in which there was zero heat transfer [$q_w = 0$], observations on friction and velocity distribution in the flow were made. This was an essential part of the work because, in addition to ascertaining correct flow conditions, the results were employed in the heat-transfer experiments and analysis. It was also possible to compare the friction and velocity data with well-established results of previous workers. Phase 2 of the programme was for the case of $\gamma = 0$, i.e. with heat transfer at the lower wall only. Finally, in the third and last phase, tests were carried out with various positive values of γ.

It was necessary to simulate as closely as possible the conditions of the idealized model. Two-dimensional flow was approximated to by means of flow in a duct of large aspect ratio. Two ducts (or channels) were employed. In phase 1, a duct of section 10 × 1 in. and 5 ft long was used. Trip wires on the roof and floor were fitted at inlet to enhance flow development and to ensure that the velocity profile at the velocity-measuring section about 4 ft downstream was fully developed. Static pressure tappings were fitted at intervals of 6 in. on the roof centre-line. A total head probe of 0·025 in. o.d. hypodermic needle, was mounted on a traversing bar which was let into and flush with the roof at the 4-ft downstream station. The body of the probe was in contact with a dial gauge so that the vertical position y could be measured to within 0·0005 in. The closest approach of the stagnation point to the floor of the channel was 0·0125 in. This arrangement permitted both transverse and vertical velocity traverses of the flow, the purpose of the transverse movement being to study the unavoidable and undesirable side-wall boundary-layer effects.

In phases 2 and 3, a second duct arrangement was employed. The 10 × 1 in. channel was unsatisfactory for heat-transfer experiments because of its relatively small length/equivalent diameter ratio. The thermal entry length is much greater than the hydrodynamic entry length, particularly when one wall is insulated, i.e. when $\gamma = 0$. Consequently, a narrower duct 9·3 × 0·32 in. and 5 ft long was constructed and this was preceded by an entry length 3 ft long. The function of the entry length was to produce fully developed flow in the heated length. The layout is shown in Fig. 2(a). An additional

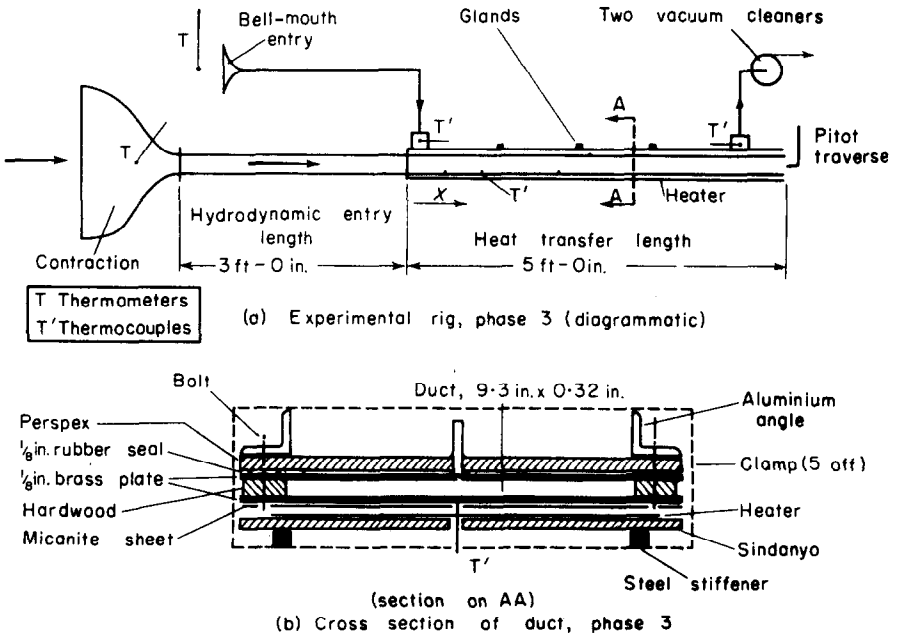

FIG. 2. Experimental rig (phase 3).

feature of the second design was the provision of four openings (or glands) through which a thermocouple probe could be inserted. The gradient of temperature in the flow direction could be determined with this arrangement (see Appendix C). The vertical dimension of the duct could also be checked by means of a depth gauge which could be inserted through the openings. In both phase 2 and phase 3, heat transfer at the lower wall or floor was effected electrically. The heater was constructed from 60 ft of nickel–chrome wire which was let into a shallow groove on the surface of a sheet of Sindanyo. The groove (and wire) ran to and fro across the whole width of the duct, the pitch between adjacent runs being $\frac{3}{4}$ in. The heater was clamped to the underside of the bottom wall of the channel and the wire insulated from the metallic surface by two sheets of micanite. Details of the duct and heater is shown in Fig. 2(b). The spacers or side walls of the channel were made of hardwood to reduce heat conduction from the lower to the upper wall to a minimum. To provide various degrees of cooling on the upper surface, i.e. variable γ, a second narrower channel was built on top of the main channel. Air was induced through this cooling space via a bell-mouth entry by means of two vacuum cleaners in parallel as shown in Fig. 2(a). Initially, water was tried as the coolant, but sealing difficulties were encountered. Furthermore, the temperature rise in the water was found to be very small, making measurement of heat extraction unreliable. The ducting and heat-transfer length were finally covered in Cosywrap fibre-glass insulation. In phase 3 of the programme, it was necessary to pre-heat the main air to provide the necessary temperature difference for heat transfer to the secondary coolant. This was done by heaters located at inlet to the main blower; later a second bank of heaters was installed in the contraction. Any desired degree of asymmetry, i.e. any particular value of γ, was obtained by trial.

3. INSTRUMENTATION

The power to the heater was measured by a wattmeter. (In the final stages of the experimental work, an A.C. Pullin dynamometer test set was used.) The electrical circuit included a resistance bank for variation of the heater load.

The environment and air-inlet temperatures were recorded on mercury-in-glass thermometers. To measure the lower-plate temperature, eight copper–constantan thermocouples were soft-soldered to the underside of the floor of the duct on the centre-line. Calculation showed that the temperature drop through the lower plate, which was $\frac{1}{8}$-in. brass, would be very small, so that the complication of the attachment of the thermojunctions to the air-side surface was avoided. The thermocouple leads were led through holes in the Sindanyo heater carrier and the micanite sheets. Fig. 2(a) shows the two thermocouples which measured the inlet and outlet coolant-air temperatures; these thermocouples were housed in mixing boxes at inlet and outlet to the secondary channel. One or two additional thermocouples were attached at the side of the duct on the lower surface to determine if the sideways conduction was significant. To measure the gradient of temperature of the main air in the flow direction, a thermocouple probe was made. The actual vertical position of the junction of the probe in the air flow was unimportant, provided that it was the same at all four measuring stations (see Appendix C). Another thermocouple, which could be attached by adhesive to the outside of the insulation, was used for the determination of heat loss to the environment (Appendix B). All e.m.f. were recorded on a Cambridge workshop potentiometer, a thermocouple selector switch and common cold junction at the melting point of ice being incorporated in the circuit. All thermocouples were manufactured from Insuglass copper and constantan wire.

In all phases of the experimental programme, static pressures and total heads were measured with an alcohol inclined manometer which could be adapted as a null-reading instrument. The reservoir of the manometer butted against a micrometer screw thus facilitating the accurate measurement of small pressures. In the heat-transfer tests, velocity traverses were made at the duct outlet to determine the mass flow and Reynolds number of the flow. The same pitot tube was used here as was employed in the adiabatic flow tests of phase 1.

The secondary air which produced the cooling of the upper wall (or roof) of the main duct was induced via a bell-mouthed entry at the inlet of a very long pipe. A static-pressure tapping was fitted at the end of the bell mouth where it joined the pipe, and the average velocity in the pipe was calculated from the recorded pressure drop below atmospheric. A mercury-in-glass thermometer near the bell-mouth entry was used to measure the room temperature in that locality.

4. EXPERIMENTAL RESULTS AND CALCULATIONS

4.1 *Adiabatic flow (no heat transfer)—phase* 1

A number of runs without heat transfer were conducted to measure static pressure and velocity distribution in the 10 × 1 in. channel. Fig. 3 shows typical results for the variation in static pressure along the centre-line of the channel. For the major part of the duct length, the pressure was linear in distance. During the commissioning period, a number of transverse static-pressure measurements were made near the outlet of the duct, which showed that the pressure decreased towards the duct corners. This was a three-dimensional effect which was associated with secondary flows in the corners.

A fairly wide range of mass flow was possible in these experiments, and a number of the vertical velocity profiles at the centre-line of the duct 4 ft downstream are shown in Fig. 4. It will be observed that good symmetry of flow was obtained over the whole range of Reynolds number. Average velocities were calculated from these profiles and related to the corresponding centre-line velocities with the result shown in Fig. 5. Included in this figure are similar results for measurements taken at the 9·3 × 0·32 in. duct outlet in the heat-transfer experiments. Subsequently, Fig. 5 was used to determine the average velocity in a test from centre-line velocity measurements. The extent of the side-wall boundary layers was determined

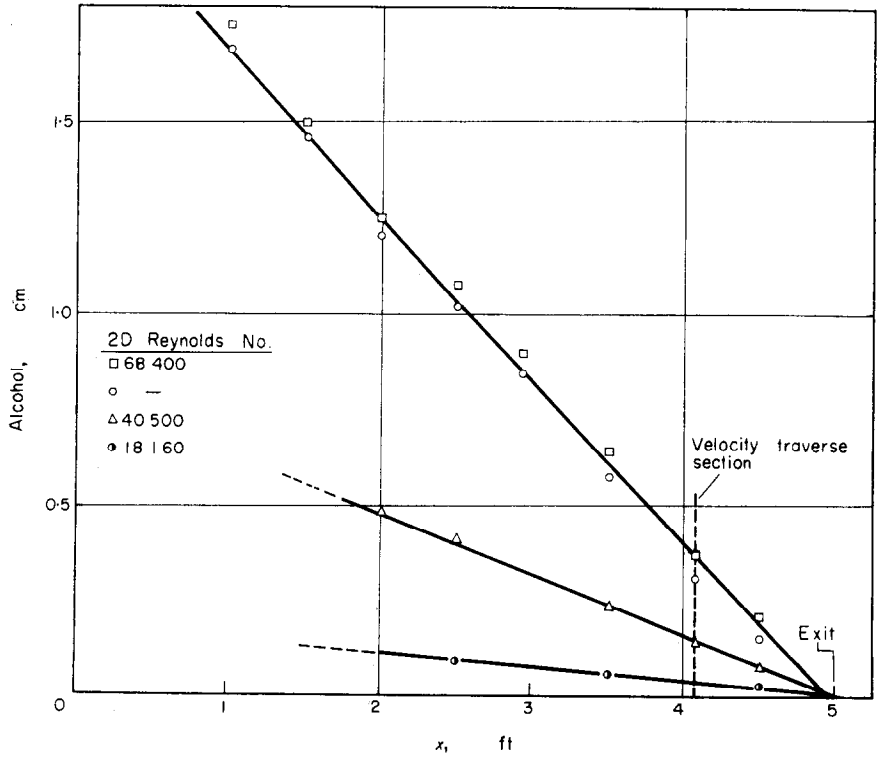

FIG. 3. Pressure distribution in channel (phase 1).

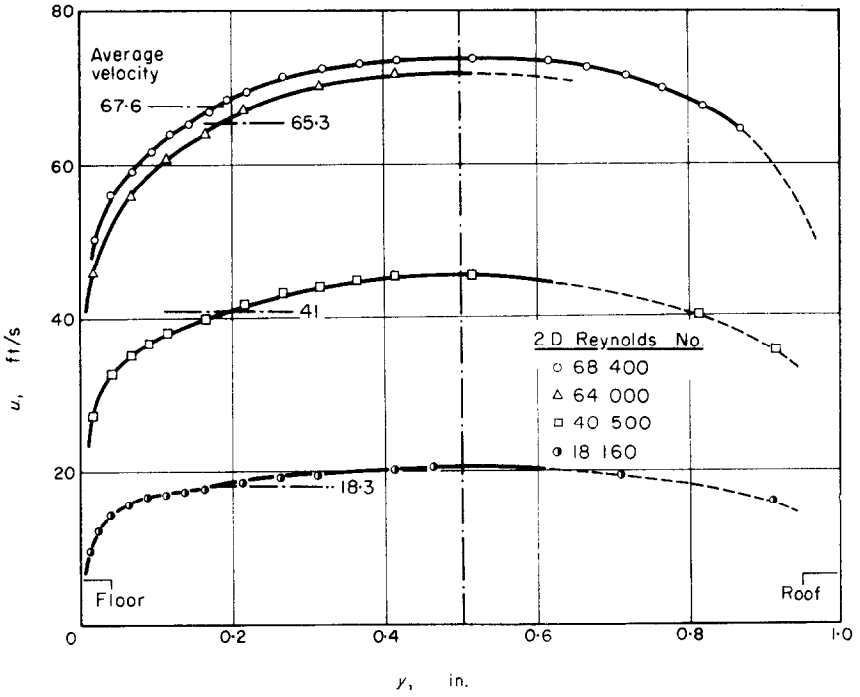

FIG. 4. Velocity profiles (phase 1).

by a transverse velocity traverse at $y = s/2$. Except for relatively narrow regions adjacent to the side walls, the velocity was uniform over the whole width of the duct. For comparison with recognized correlating equations for velocity distribution, the velocity data were plotted as generalized velocity profiles as shown in Figs. 6–8. This was done on both the channel and two-dimensional bases, i.e. the wall friction τ_w (and friction velocity u_τ) was calculated respectively from

$$\tau_w = \left(\frac{dp}{dx}\right)\left(\frac{A}{P}\right) \tag{1}$$

and

$$\tau_w = \left(\frac{dp}{dx}\right)\left(\frac{s}{2}\right) \tag{2}$$

the pressure gradient being determined from the centre-line static-pressure measurements. Clearly, as the aspect ratio of the duct section increases, τ_w calculated from equation (1) becomes almost equal to τ_w calculated from equation (2), which is that for the idealized model, Fig. 1. In the present case, the difference is marked and this becomes evident if comparison is made between Figs. 6 and 7. The results on the two-dimensional basis show better agreement with the Prandtl–Nikuradse, Deissler [3], Knudsen and Katz [4], and Corcoran *et al.* [5] recommendations. As is usual, the experimental points close to the wall (or channel floor) are too high (see Fig. 8). Within the instruments available, only a limited amount of data was obtainable in this region.

It was concluded that this preliminary investigation was entirely satisfactory and the results and techniques could be used with confidence in the heat transfer work. The equations of Corcoran *et al.* [5] are preferred for reasons given in Appendix A.

4.2 *Heat transfer*—$\gamma = 0$—*phase* 2

The heat-transfer experiments were carried out with the 9·3 × 0·32 in. duct; in the second phase of the programme the upper surface was

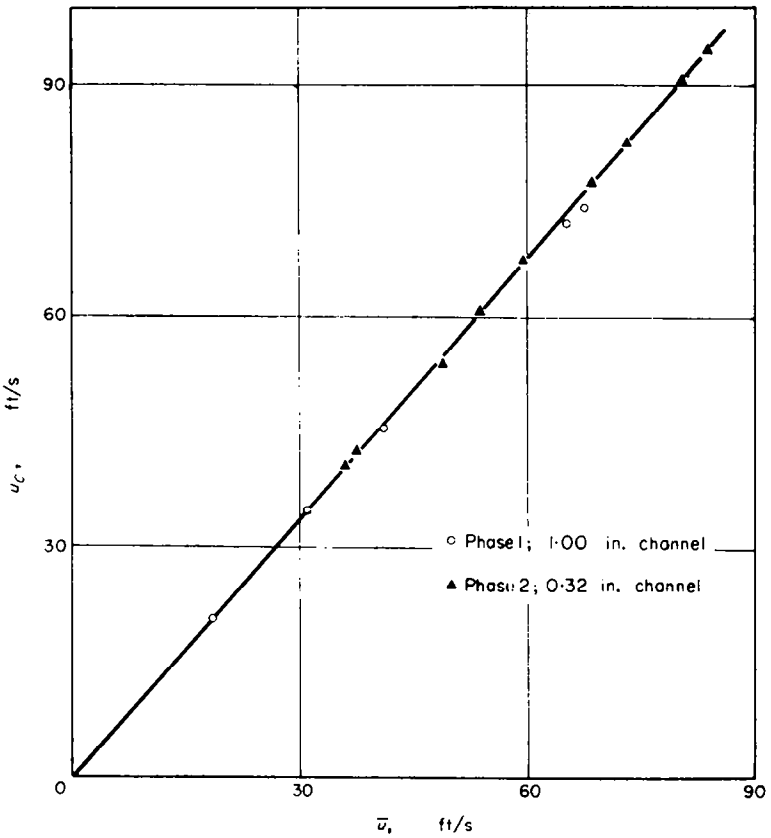

FIG. 5. Relation between average velocity $\bar{u}$, and centre-line velocity u_c.

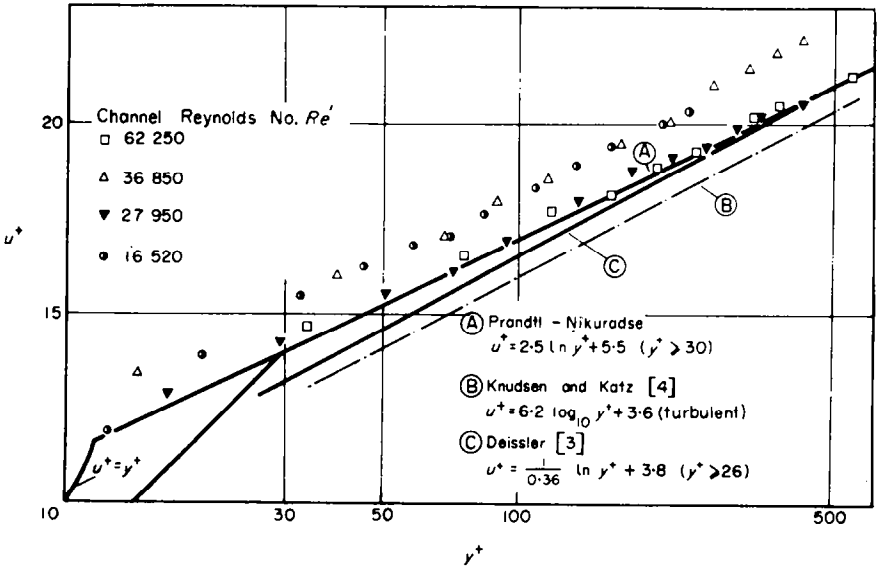

FIG. 6. Velocity distribution (phase 1, channel basis).

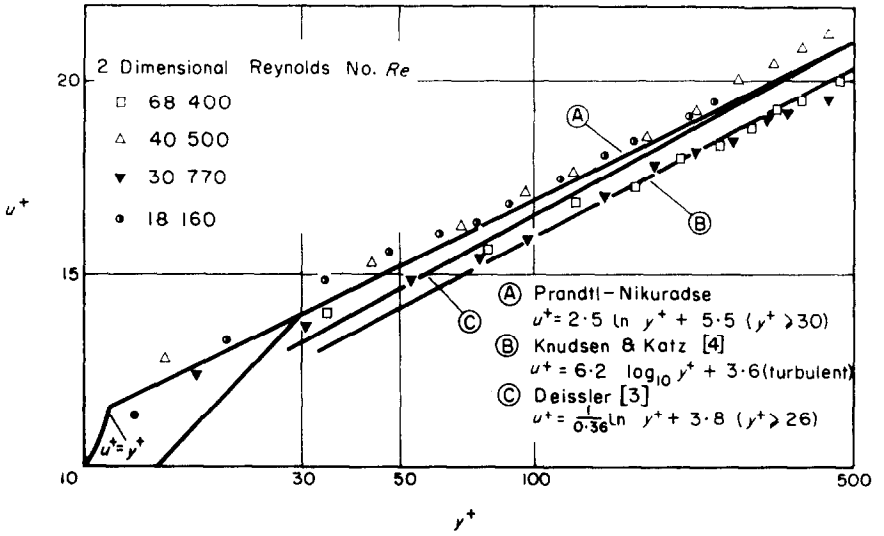

FIG. 7. Velocity distribution (phase 1, two-dimensional basis).

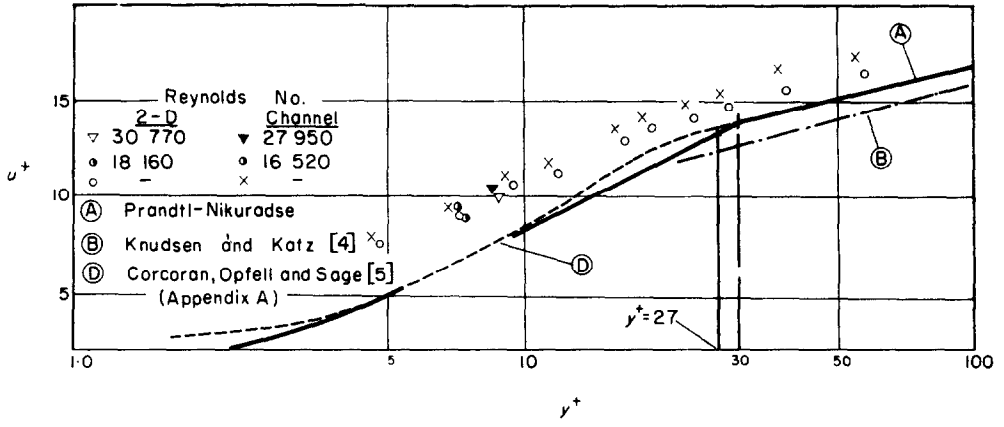

FIG. 8. Velocity distribution near channel floor (phase 1).

insulated, i.e. $\gamma = 0$. For various values of the mass velocity G and the wall heat flux q_w, the following measurements were made after steady state conditions had been obtained:

(i) Environment (or ambient) temperature, T_a;
(ii) Wall temperature, T_w;
(iii) Air inlet temperature, T_i;
(iv) Insulation surface temperature, T_s;
(v) Heater power;
(vi) Probe thermocouple temperature, T;
(vii) Centreline velocity at outlet, u_c;
(viii) Static pressure, p.

With $\gamma = 0$, pre-heating of the air was unnecessary, and in all runs T_i differed only slightly from T_a

Figure 9 shows the friction results of this series of tests as Fanning friction factor f against the Reynolds number, both parameters being evaluated on the two-dimensional basis. The employment of a duct of much higher aspect ratio in phase 2 made τ_w as calculated from equations

(1) and (2) almost identical. The Blasius relation $f = 0{\cdot}079\ Re^{-1/4}$ for tube flow is shown for comparison on the understanding that the hydraulic radius concept is applicable. In many instances of flow in non-circular ducts, the friction factor f is frequently too high, and these results are typical. However, the correlation is considered satisfactory, the scatter of the points being attributed to the difficulty of measuring small pressure differences. The Blasius relation is used in the heat-transfer analysis given in the Appendix A.

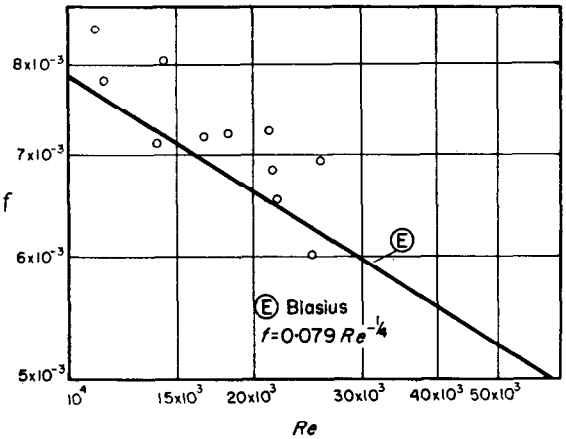

FIG. 9. Friction factors (phase 2).

To measure the heated-wall heat-transfer coefficients, the heat flux q_w, wall temperature T_w and air bulk temperature T_B are required. When the value of h at a particular value of x is required, the local values of q_w, T_w and T_B are used. The wall temperature is measured directly and Fig. 10 shows its variation in the test at $Re = 25{,}800$. Thermal entry and exit effects exist where shown. The wall temperatures are those on the centre-line, and a number of temperature measurements across the plate showed a decrease towards the corners. This departure from the two-dimensional was unavoidable. The bulk temperature of the air was determined in two ways. Heat losses were first determined as outlined in Appendix B and deducted from the electrical power input. The net heat input was then equated to the enthalpy increase, and the final air temperature calculated. Alternatively, the bulk temperature was determined by measuring the gradient of the air temperature at an arbitrary value of y.

The thermocouple probe was located in the main air stream by passage of it through the glands. The probe readings were collinear when plotted against x, and a line of the same slope was drawn through the inlet temperature point to obtain the locus of the bulk temperature. Appendix C describes the validity of this technique and how it may be used to calculate heat transfer to the air. The fact that the thermocouple readings were linear in distance indicated that the heat flux q_w was uniform lengthwise. In all cases, the air temperature calculated in this way was lower than that determined from the electrical-power and heat-loss data. This was attributed to the possibility of underestimating the heat losses. The results of the calculation made in the two ways are shown in Fig. 10.

To calculate the heat-transfer coefficient h, the following equation is used

$$h = \frac{q_w}{(T_w - T_B)}. \tag{3}$$

$(T_w - T_B)$ was observed to decrease with length x outside the entry and exit regions, which means that, for q_w constant, h increases with x. Deissler [6] predicts this to be the case, but his reasons cannot be used to explain this observation in the present experiments. Three-dimensional effects are obviously present and these might enhance the increase in heat-transfer coefficient as x increases. In these circumstances, average conditions were taken at about $x/D_e = 50$ and the heat-transfer coefficient determined at that point. The overall result is presented in Fig. 11. The experimental results for $\gamma = 0$ on both methods of calculation are compared with the theoretical predictions which are derived in Appendix A. The dimensional analysis result $Nu = 0{\cdot}02\ Re^{0{\cdot}8}$ has been included. The following observations were made:

(i) The experimental heat-transfer coefficients were less than the predicted and accepted result, $Nu = 0{\cdot}02\ Re^{0{\cdot}8}$ for symmetrical heating, $\gamma = -1$.
(ii) The experimental heat-transfer coefficients based on electric-power and

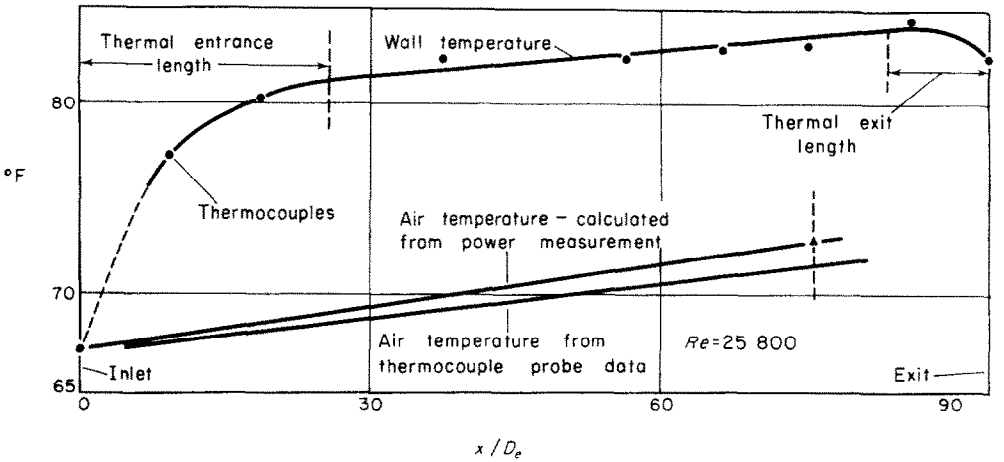

FIG. 10. Typical longitudinal-wall and air-temperature profiles (phase 2).

thermocouple-probe readings were respectively greater and less than the theoretical values for $\gamma = 0$. [Those results calculated from electrical power measurements are probably too high as a result of underestimation of the heat losses. With increased heat losses, q_w is smaller, $(T_w - T_B)$ is larger and hence h is smaller according to equation (3).]

(iii) The scatter of the experimental points was wide. This would tend to prevent any distinction being made between results for $\gamma = 0$ and future results for $\gamma = +1$ (and intermediate values) by this direct method of measuring heat-transfer coefficient.

4.3 *Heat transfer—variable γ—phase* 3

As described previously in section 2, experiments with γ ranging from 0 to $+1$ were conducted with the same duct as in phase 2. Cooling at the upper surface was produced by a secondary air flow. These experiments were run as follows:

With no secondary air, i.e. $\gamma = 0$, the apparatus was operated exactly as in phase 2, but with the inlet temperature elevated by supply of heat at the fan inlet. The same readings as listed in section 4.2 were recorded. Cooling of the upper surface was then effected by operation of the secondary air circuit, and, when steady conditions were re-established, the readings were repeated. In addition, the bell-mouth pressure measurement and secondary air inlet and outlet temperatures were noted. In the earlier tests of this kind, thermocouple probe readings were taken with and without heat transfer at the upper surface; the purpose of these measurements is explained in Appendix D.

Typical wall temperatures for this series of tests are shown in Fig. 12. In all cases, there was a reduction in the temperature of the lower wall when the upper wall was cooled. With $\gamma = 0$, the air-bulk temperature was calculated as outlined previously on the basis that the heat supplied to the air equalled the electrical power less the heat losses.

To determine the main air temperature profile with cooling at the upper surface, the heat transfer to the main fluid was first calculated from the difference between the heat equivalent of the electrical power (less losses) and the heat extraction at the upper surface. The heat transfer at the upper surface was determined from the enthalpy increase of the secondary air i.e. the secondary air mass flow times the temperature rise, times the specific heat. (This method of calculation was more reliable in this series of experiments than that which used the gradient of the main air temperature as determined by the thermocouple probe.) The net heat

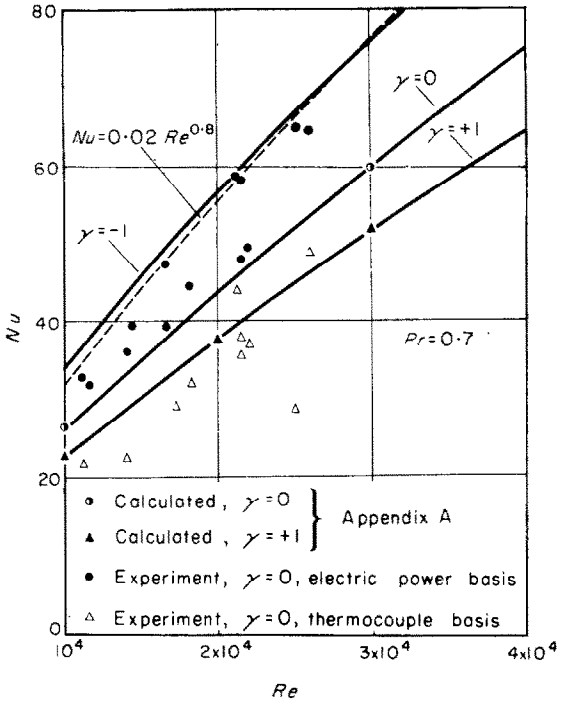

FIG. 11. Heated-wall heat-transfer coefficients (phase 2).

transfer was then equated to the enthalpy increase of the main air and the final temperature evaluated. The longitudinal profile of the bulk temperature T_B is shown in Fig. 12.

The value of γ which equals the heat transfer at the upper surface divided by the heat transfer at the lower surface is, of course, an average one. This is because the difference between the temperature of the main and secondary air flows varies with length. The effect was more significant at the high values of γ and the variation of γ with length was kept to a minimum by use of large temperature differences and large secondary air mass flow.

In order to study the effect of variable γ on the lower wall heat-transfer coefficient, the ratio $Nu/Nu_{\gamma=0}$ was calculated for different degrees of cooling at approximately constant Reynolds number. The previous analysis [2] shows that this ratio is only a weak function of the Reynolds number and consequently would not change significantly over the Reynolds-number range of these experiments; furthermore, it was anticipated that inaccuracies in the experimental work would mask such a dependency. A Reynolds number of about 16000 was selected, although the choice was governed to some extent by the facilities available. A number of tests were run and in each case the ratio $Nu/Nu_{\gamma=0}$ was calculated from the equation

$$\frac{Nu}{Nu_{\gamma=0}} = \frac{(T_w - T_B)_{\gamma=0}}{(T_w - T_B)}. \tag{4}$$

An examination of Fig. 12 shows that this ratio is a function of position, so that its value at a number of values of (x/D_e) (away from the entry and exit regions) was calculated. The results are presented as a plot of $Nu/Nu_{\gamma=0}$ against γ in

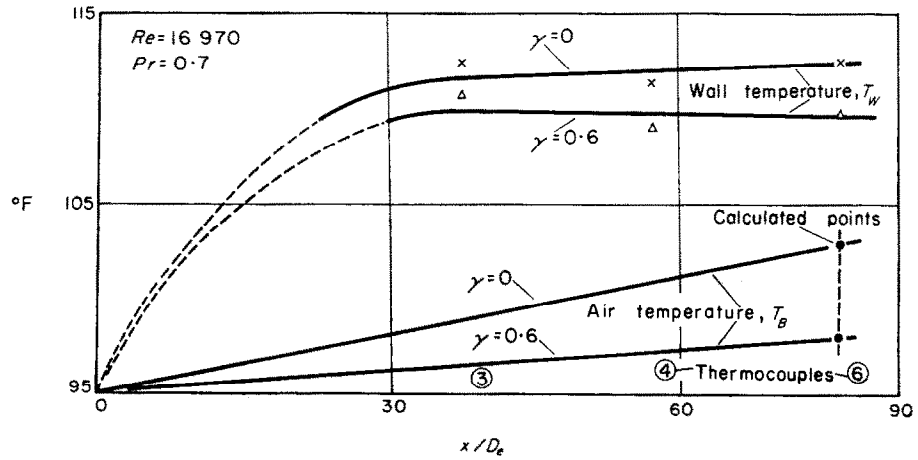

FIG. 12. Typical longitudinal-wall and air-temperature profiles (phase 3).

Fig. 13. The predictions of the previous analysis [2] and that given in Appendix A are included. In the latter analysis, a linear relation between $Nu/Nu_{\gamma=0}$ is assumed for plotting purposes, since only the extreme cases $\gamma = 0$ and $\gamma = +1$ were calculated. This is a safe assumption, because intermediate values may be determined on the simple theory and in that case the relationship is approximately linear as shown. All the experimental points have been included in the plot. The most important observation to

5. DISCUSSION AND CONCLUSIONS

Experiments have been carried out to study turbulent flow of air between smooth parallel plates and the effect of unequal wall heat fluxes on the convective coefficients of heat transfer.

The friction and velocity data for turbulent flow in channels of large aspect ratio which were used to simulate two-dimensional flow were satisfactorily correlated by accepted relationships.

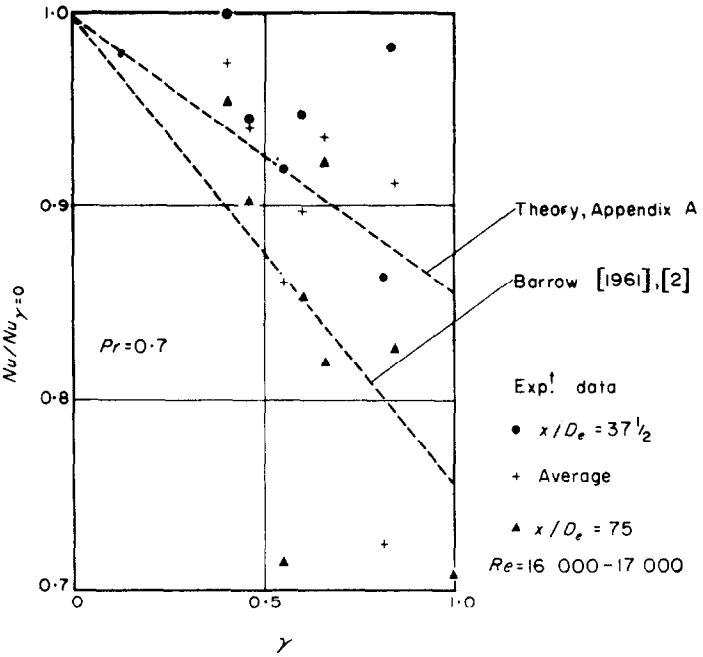

FIG. 13. Variation at heated-wall heat-transfer coefficient, Nu with asymmetry parameter γ (phase 3).

be made is that, in general, the experimental heat-transfer coefficient decreases as γ increases from zero to unity. The scatter is marked, but agreement between experiment and theory is readily apparent. The temperature differences in equation (4) are small so that small errors in measuring the wall temperature and in calculating the air bulk temperature can lead to relatively large errors in the value of $Nu/Nu_{\gamma=0}$. This is probably the main cause of the scatter of the experimental data; operation with higher heat fluxes would reduce this.

The heat-transfer results for asymmetrical heat transfer showed that the heat-transfer coefficient is a function of heat-flux distribution (around the flow section) and the Reynolds number of the flow. For a given Reynolds number, the heat-transfer coefficient decreases as the asymmetry parameter γ increases up to unit value. A variation of heat-transfer coefficient with position in the developed region was observed, and this might be attributed to parasitic three-dimensional effects. These effects are considered to have been one of the main

causes of the scatter of the experimental data.

A more rigorous theoretical study has been made (Appendix A). One of the improvements of this analysis over the previous work [2] is clearly shown in Fig. 14. For $\gamma = +1$, i.e. steady adiabatic flow with heat transfer, the temperature profile is unrealistic when calculated according to [2], while on the new theory it is similar to the experimental temperature profile of Page *et al.* [7]. Further improvement in the theory is possible and will be necessary in cases where the diffusivities of heat and momentum are unequal. The equality of ϵ_H and ϵ_M for all y and Re has been assumed in the present analysis, and this is an oversimplification. (The data of Page *et al.* [7] show a marked difference between ϵ_H and ϵ_M even for gas flow.) For lower Prandtl numbers particularly, (ϵ_H/ϵ_M) can no longer be considered to be equal to unity, but must be expressed as a function of both wall distance and Reynolds number. Allowance for this variation will have to be made in the analysis when the Prandtl-number effect is studied.

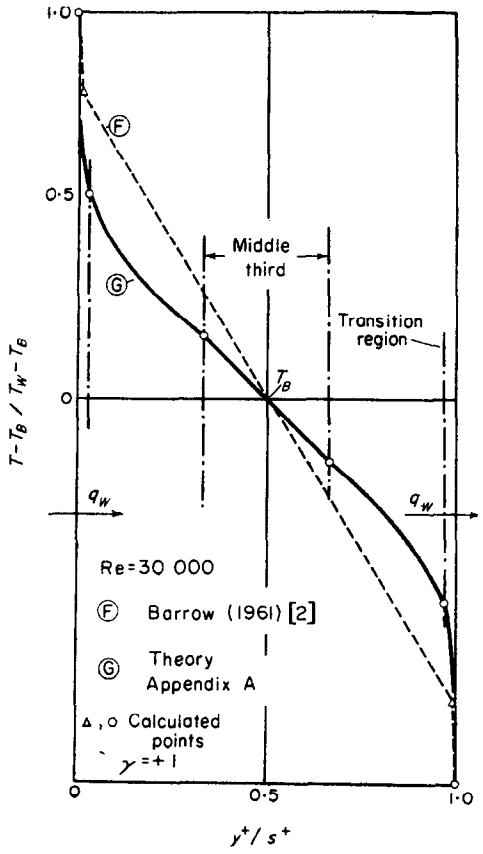

FIG. 14. Theoretical air temperature profiles, $\gamma = +1$.

The agreement between the theory and practice is only fair, but, in view of the difficulties in experimentation of this nature, the results of the work are satisfactory. Unlike the previous analysis [2] which results in a simple working formula, the present theoretical study which is more thorough will require extensive numerical computation before it can be applied directly to engineering problems.

In conclusion, the dependency of local heat-transfer coefficient on heat-flux distribution around the flow section has been verified: in general, it is less than that for symmetrical heating at the same Reynolds number of the flow.

ACKNOWLEDGEMENT

The author wishes to thank Professor J. H. Horlock for permission to use the workshop and laboratory facilities in the Department of Mechanical Engineering, The University of Liverpool.

REFERENCES

1. H. BARROW, An observation on the use of dimensional analysis and similarity relations in non-uniform heat transfer. *J. Roy. Aero. Soc.* **65**, 505–507 (1961).
2. H. BARROW, Convection heat transfer coefficients for turbulent flow between parallel plates with unequal heat fluxes. *Int. J. Heat Mass Transfer*, **1**, 306–311 (1960).
3. R. G. DEISSLER, Analytical and experimental investigation of adiabatic turbulent flow in smooth tubes. *N.A.C.A.* TN 2138 (1950).
4. J. G. KNUDSEN and D. L. KATZ, Fluid dynamics and heat transfer. *Bull. Inst. Engng Res. Univ. Mich.* No. 37, p. 61 (1953).
5. W. H. CORCORAN, J. B. OPFELL and B. H. SAGE, *Momentum Transfer in Fluids.* Academic Press, New York (1956).
6. R. G. DEISSLER, Analysis of turbulent heat transfer and flow in entrance regions of smooth passages. *N.A.C.A.* TN 3016 (1953).
7. F. PAGE, JR., W. G. SCHLINGER, D. K. BREAUX and B. H. SAGE, Temperature gradients in turbulent gas streams—Point values of eddy conductivity and viscosity in uniform flow between parallel plates. *Industr. Engng Chem.* **44**, 424 (1952).
8. M. FISHENDEN and O. A. SAUNDERS, *An Introduction to Heat Transfer.* Clarendon Press, Oxford (1950).

APPENDIX A

Improved Correlation of Heat-Transfer Results

The previous theoretical analysis of the present author [2] serves to illustrate the dependence of heat transfer at a point on a wall on the variation of heat transfer around the boundary of the cross-section through which a fluid flows. This simple theory makes the following assumptions:

(i) A finite laminar sub-layer;
(ii) constant turbulent diffusion, ϵ in the main stream.

Both these assumptions are oversimplifications, because in reality a sublayer does not exist and the turbulence effects vary across the stream and vanish at the boundary of the flow. Regions near the boundary where ϵ is small offer the greatest resistances to heat transfer and therefore a knowledge of the flow near the boundary is important.

For fully developed turbulent flow between parallel plates, the recommendations of Corcoran *et al.* [5] will be used, for they allow for a gradual decay of turbulence as the wall is approached and a more realistic variation of turbulent diffusion across the stream. In the transition region near the wall, $0 \leqslant y^+ \leqslant 27$ and

$$u^+ = \frac{1}{0{\cdot}0695} \tanh (0{\cdot}0695\, y^+) \qquad \text{(A1)}$$

and in the fully turbulent region

$$u^+ = 5{\cdot}5 + 2{\cdot}5 \ln y^+. \qquad \text{(A2)}$$

(Note that the first derivatives of these relationships are equal at $y^+ = 27$.) From these equations, the eddy diffusivity ϵ may be determined using

$$(\epsilon + \nu) = \frac{\tau_w}{\rho}\left[1 - \frac{2y}{s}\right] \Big/ \frac{\mathrm{d}u}{\mathrm{d}y}. \qquad \text{(A3)}$$

In the fully turbulent region, the velocity distribution given above predicts zero ϵ at the channel centre. Corcoran *et al.* recommend using a constant value of ϵ over the middle third of the channel (this constant value is that calculated at the point $y/s = 1/3$). The expressions for the turbulent momentum diffusion coefficient are as follows:

$$\left.\begin{aligned} &\text{(i)}\ 0 \leqslant y^+ \leqslant 27,\ \epsilon = \left[1 - \frac{2y^+}{s^+}\right] [\nu \cosh^2 (0{\cdot}0695\, y^+)] - \nu \\ &\text{(ii)}\ 27 \leqslant y^+ \leqslant \frac{s^+}{3},\ \epsilon = \left[1 - \frac{2y^+}{s^+}\right]\left(\frac{y^+\nu}{2{\cdot}5}\right) - \nu \\ &\text{(iii)}\ \frac{s^+}{3} \leqslant y^+ \leqslant \frac{s^+}{2},\ \epsilon = \frac{s^+\nu}{22{\cdot}5} - \nu. \end{aligned}\right\} \qquad \text{(A4)}$$

It will be assumed that these expressions describe the distribution of the eddy diffusivity for heat also and may be used directly in the governing heat-transfer equation

$$\frac{q}{c\rho} = -(\epsilon + \alpha)\frac{\partial T}{\partial y}. \qquad \text{(A5)}$$

Then, if q is a known function of y, the temperature may be determined and the heat-transfer coefficient calculated. This procedure will be applied to various problems and the results will be compared with the predictions of the more simple theory and the experimental heat-transfer data of the present investigation.

Case 1—*symmetrical heating* ($\gamma = -1$)

In this case

$$q = q_w\left(1 - \frac{2y}{s}\right) \qquad \text{(A6)}$$

approximately. Therefore, we may use equation (A5) to determine the temperature as follows:

Between the wall and $y^+ = 27$, the temperature difference $(T_w - T_1)$ is

$$(T_w - T_1) = \frac{q_w Pr}{c\,\rho\,u_\tau} \int_0^{27} \frac{(1 - 2y^+/s^+)\,\mathrm{d}y^+}{Pr \cosh^2 (0{\cdot}0695\, y^+)[1 - (2y^+/s^+)] - (Pr - 1)} \qquad \text{(A7)}$$

or, ignoring the small variations in shear stress and heat flux in this region, i.e. $y^+ \ll s^+$,

$$(T_w - T_1) = \frac{q_w Pr}{c \rho u_\tau}$$

$$\int_0^{27} \frac{dy^+}{Pr \cosh^2 (0{\cdot}0695\, y^+) - (Pr - 1)} = \frac{q_w Pr}{c \rho u_\tau} I,$$

where

$$I = \int_0^{27} \frac{dy^+}{Pr \cosh^2 (0{\cdot}0695\, y^+) - (Pr - 1)}. \quad (A9)$$

In the turbulent region, i.e. for $y^+ > 27$, the Reynolds analogy may be used, because τ and q are similar functions of y in this case. The difference between the temperature at the $y^+ = 27$ position and the bulk temperature is

$$T_1 - T_B = \frac{q_w}{c \tau_w} [\bar{u} - u_1]. \quad (A10)$$

Adding equations (A9) and (A10) we get the total temperature difference:

$$T_w - T_B = \frac{q_w}{c} \left[\frac{\bar{u} - u_1}{\tau_w} + \frac{Pr\, I}{\rho u_\tau} \right] \quad (A11)$$

and the heat transfer coefficient is given by

$$Nu = \frac{Re\, Pr\, q_w}{c \rho \bar{u} (T_w - T_B)}. \quad (A12)$$

The experiments connected with this report were carried out using air when $Pr = 0{\cdot}7$. The integral I can be evaluated graphically and is found to be 15·2. Substitution of these values in the temperature difference, $(T_w - T_B)$ and with $u_\tau = 0{\cdot}1986\, \bar{u}\, Re^{-1/4}$ (Blasius), gives the heat-transfer coefficient as

$$Nu = \frac{0{\cdot}139\, Re^{7/8}}{5{\cdot}03\, Re^{-1/8} - 3{\cdot}06} \quad (Pr = 0{\cdot}7). \quad (A13)$$

Equation (A13) is shown in Fig. 11. The improved theory follows more closely the line representing the well-established equation

$$Nu = 0{\cdot}023\, Re^{0{\cdot}8}\, Pr^{0{\cdot}4} = 0{\cdot}02\, Re^{0{\cdot}8}$$

particularly in the higher range of Re.

Case 2—Wall heat fluxes of equal magnitude but of opposite sign ($\gamma = +1$)

Here $q = q_w = \text{const}$ and the temperature distribution is as follows:

(i) $$(T_w - T_1) = \frac{Pr\, q_w}{c \rho u_\tau}$$

$$\int_0^{27} \frac{dy^+}{[Pr\,(1 - 2y^+/s^+) \cosh^2 (0{\cdot}0695\, y^+) - (Pr - 1)]}, \quad (A14)$$

(ii) between the positions where $y^+ = 27$ and $y = s/3$ the temperature difference $(T_1 - T_2)$ is

$$(T_1 - T_2) = \frac{Pr\, q_w}{c \rho u_\tau}$$

$$\int_{27}^{s^+/3} \frac{dy^+}{[(1 - 2y^+/s^+)(y^+/2{\cdot}5)\, Pr - (Pr - 1)]}; \quad (A15)$$

(iii) the difference between the temperature at $y = s/3$ and the temperature at $y = s/2$ is $(T_2 - T_B)$, because at $y = s/2$ the temperature is the bulk temperature T_B.

Therefore,

$$(T_2 - T_B) = \frac{q_w Pr}{c \rho u_\tau [Pr\, s^+/22{\cdot}5 - (Pr - 1)]} \int_{s^+/3}^{s^+/2} dy^+ \quad (A16)$$

$$(T_2 - T_B) = \frac{q_w Pr\, s^+}{6c \rho u_\tau [Pr\, s^+/22{\cdot}5 - (Pr - 1)]}. \quad (A17)$$

Summing the individual temperature differences

$$(T_w - T_B) = \frac{q_w Pr}{c \rho u_\tau} [I_1 + I_2 + I_3] \quad (A18)$$

where

$$I_1 = \int_0^{27} \frac{dy^+}{[Pr\,(1 - 2y^+/s^+) \cosh^2 (0{\cdot}0695\, y^+) - (Pr - 1)]} \quad (A19)$$

which equals 15·2 for $Pr = 0{\cdot}7$ (see case 1), and

$$I_2 = \int_{27}^{s^+/3} \frac{dy^+}{(1 - 2y^+/s^+)(y^+/2{\cdot}5)\, Pr - (Pr - 1)} \quad (A20)$$

On rearrangement of the denominator, this integral may be evaluated directly. The factor $(1 - 2y^+/s^+)$ must be included in this integral for it no longer approximates to unity. Therefore,

$$I_2 = \frac{0{\cdot}625\, s^+}{Pr\,\sqrt{\{[(1-Pr)/Pr]\,1{\cdot}25\, s^+ + s^{+2}/16\}}} \cdot \ln\left[\frac{27 - s^+/4 - \sqrt{\{[(1-Pr)/Pr]\,1{\cdot}25\, s^+ + s^{+2}/16\}}}{27 - s^+/4 + \sqrt{\{[(1-Pr)/Pr]\,1{\cdot}25\, s^+ + s^{+2}/16\}}} \times \frac{s^+/12 + \sqrt{\{[(1-Pr)/Pr]\,1{\cdot}25\, s^+ + s^{+2}/16\}}}{s^+/12 - \sqrt{\{[(1-Pr)/Pr]\,1{\cdot}25\, s^+ + s^{+2}/16\}}}\right]. \quad \text{(A21)}$$

As before

$$I_3 = \frac{s^+}{6\,[(Pr\, s^+/22{\cdot}5) - (Pr - 1)]}. \quad \text{(A22)}$$

The heat-transfer coefficient Nu is given by

$$Nu = \frac{Re\, Pr\, q_w}{c\,\rho\,\bar{u}(T_w - T_B)} \quad \text{(A23)}$$

which may be evaluated on substitution of $Pr = 0{\cdot}7$ in the expression for the temperature difference $(T_w - T_B)$. The result is shown in Fig. 13 and indicates that the previous theory predicts a coefficient which is too small. Fig. 14 shows a typical temperature profie when $\gamma = +1$. The discontinuity occurring at $y = s/3$ is a result of the assumption of constant ϵ over the middle third of the channel.

Case 3—*One wall of the channel insulated* ($\gamma = 0$)

The position of the bulk temperature T_B in this case is not readily determined. The procedure is to calculate the overall temperature difference between the two walls, and then to calculate the ratio $[(T_w - T_0)/(T_w - T_B)]$ from the velocity and temperature distributions.

$$\left(\frac{T_w - T_B}{T_w - T_0}\right) = \int_0^1 \left(\frac{u}{u_c}\right)\left(\frac{T_w - T}{T_w - T_0}\right) \mathrm{d}\left(\frac{y^+}{s^+}\right) \Big/ \int_0^1 \left(\frac{u}{u_c}\right) \mathrm{d}\left(\frac{y^+}{s^+}\right). \quad \text{(A24)}$$

The temperature profile across the channel is determined in a manner identical to that employed in the previous cases. The heat flux q is assumed to be linear in y, and hence

$$q = q_w\left[1 - \frac{y}{s}\right] \quad \text{(A25)}$$

(at $y = s$, $q = 0$). The expression for the heat-transfer coefficient for the heated wall when $\gamma = 0$ is written as

$$Nu = \frac{Re\, Pr\, q_w}{c\,\rho\,\bar{u}(T_w - T_0)} \cdot \left(\frac{T_w - T_0}{T_w - T_B}\right) \quad \text{(A26)}$$

or

$$Nu = \frac{0{\cdot}1986\, Re^{7/8}}{I_1 + I_2 + I_3 + I_4} \cdot \left(\frac{T_w - T_0}{T_w - T_B}\right) \quad \text{(A27)}$$

where

$$\left.\begin{aligned} I_1 &= \int_0^{27} \frac{(1 - y^+/s^+)\,\mathrm{d}y^+}{Pr\,\cosh^2(0{\cdot}0695\, y^+)\,(1 - 2y^+/s^+) - (Pr - 1)} \\ I_2 &= \int_{27}^{s^+/3} \frac{(1 - y^+/s^+)\,\mathrm{d}y^+}{(1 - 2y^+/s^+)\,(y^+\, Pr/2{\cdot}5) - (Pr - 1)} \\ I_3 &= \frac{s^+}{6\,[Pr\, s^+/22{\cdot}5 - (Pr - 1)]} \\ I_4 &= \int_{27}^{+\,/3} \frac{(y^+/s^+)\,\mathrm{d}y^+}{(1 - 2y^+/s^+)\,(y^+/2{\cdot}5)\,Pr - (Pr - 1)}. \end{aligned}\right\} \quad \text{(A28)}$$

The temperature drop across the transition region adjacent to the insulated wall is very small and is ignored because little heat reaches this region. The calculation made in this way will result in a heat-transfer coefficient which is intermediate between those predicted for the $\gamma = +1$ and $\gamma = -1$ cases.

The foregoing analyses are expected to cover a wider range of Prandtl number, in addition to increasing the Reynolds number range. If ϵ_H and ϵ_M differ widely, account of this could be taken in making the calculation. However, since (ϵ_H/ϵ_M) is a function of both y and Re, the algebra becomes unmanageable. Experiments with a wide range of different fluids will be required to determine the dependence of asymmetrical heat transfer on Prandtl number.

APPENDIX B

Heat Losses

For determining the true heat transfer to the air in the experiments reported here, heat losses must be estimated and deducted from the electric-power input. Heat losses are significant when the heat fluxes are small, as was the case here. The total heat loss to the environs comprises conduction, natural convection and radiation components. The former arises because of the attachment of the heat experimental length of duct to the entry length, and can be determined from the slope of the axial temperature gradient in the duct at the point of attachment. The natural convection and radiation losses from the duct to the environs are $CA_s(T_s - T_a)^{5/4}$ and $\sigma A_s e(T_s^4 - T_a^4)$ respectively. The constant C varies according to whether the surface is vertical or horizontal (facing upwards or facing downwards); see for example Reference [8].

The observations necessary include the insulation surface temperature T_s and the ambient temperature T_a. The former was measured with a thermocouple attached to the surface. Estimates made in this way, indicate that the total heat loss was of the order of 10 per cent of the electric power supplied to the heater.

When only one wall is heated, thermal conduction to the opposite wall via the sides takes place. This was kept to a minimum by the use of hardwood material for the side walls, as described earlier in section 2. The conduction by this path is not a heat loss, but under these conditions γ is not strictly equal to zero.

APPENDIX C

An Alternative Method for the Measurement of Heat Transfer to the Air Flow

An alternative to the measurement of electric-power input (less heat losses) for the calculation of the heat transfer to the air is the use of a thermocouple probe. From steady-flow energy considerations, the heat transfer in the fully developed hydrodynamic and thermal-flow region equals the increase in enthalpy of the air.

Considering unit width of duct and two-dimensional flow,

$$q_w \, \delta x = G s c \, \delta T_B. \qquad \text{(C1)}$$

Clearly a measurement of bulk temperature T_B in the direction x will give q_w. Furthermore, if T_B increases linearly, then q_w must be uniform, the verification of which is not possible using the electrical measurements alone. It may be shown that the gradient of the bulk temperature equals the gradient of the temperature at constant wall distance when the heat flux is constant, i.e.

$$\frac{\partial T_B}{\partial x} = \frac{\partial T}{\partial x} \neq F(y). \qquad \text{(C2)}$$

Therefore, provided that the depth of immersion of the junction of a thermocouple probe is constant, the gradient of the recorded temperature in the flow direction will be equal to the gradient of the bulk temperature. The heat flux q_w is then calculated from equation (C1), the mass flow velocity G being determined from the velocity-profile measurements.

Another advantage of the probe technique is that the temperature data are those far from the side walls in regions where the flow approximates most closely to a two-dimensional one.

APPENDIX D

Alternative Method of Determining the Heated-Wall Heat-Transfer Coefficient for the Cases when $\gamma \neq 0$

The alternative method of determining the heat transfer with a thermocouple probe (Appendix C) may be adopted in cases when

$\gamma \neq 0$. By the technique outlined here, the heat-transfer coefficient for a given asymmetry of heat transfer, i.e. for a given value of γ, may be compared with that for the special case of $\gamma = 0$.

If we consider the ideal situation, when both the wall heat fluxes, q_w and γq_w, are constant in the flow direction, Fig. 1, then, with constant fluid properties, the heat transfer equals the enthalpy increase, i.e.

$$q_w - \gamma q_w = \bar{u}\,\rho\,s\,c\left(\frac{\partial T_B}{\partial x}\right). \tag{D1}$$

When the upper surface is adiabatic, then $\gamma = 0$, and

$$q_w = \bar{u}\,\rho\,s\,c\left(\frac{\partial T_B}{\partial x}\right)_{\gamma=0} \tag{D2}$$

when

$$\gamma = 1 - \left(\frac{\partial T_B}{\partial x}\right)\Big/\left(\frac{\partial T_B}{\partial x}\right)_{\gamma=0}. \tag{D3}$$

The lower-wall heat flux is assumed constant in both cases. Therefore the γ value may be determined from the two experimental temperature gradients along the ducts according to equation (D3).

The heat transfer coefficient in the general case when $\gamma \neq 0$ is determined from

$$\frac{Nu}{Nu_{\gamma=0}} = \frac{(T_w - T_B)_{\gamma=0}}{(T_w - T_B)} \tag{D4}$$

where T_w and T_B are respectively the local-wall and fluid bulk temperatures. The lower-wall heat flux q_w is assumed the same in both cases, i.e. when $\gamma = 0$ and when $\gamma \neq 0$. Since, in general, $T_B = T_i + x(\partial T_B/\partial x)$ at any section x,

$$\frac{Nu}{Nu_{\gamma=0}} = \frac{[T_w - T_i - x(\partial T_B/\partial x)]_{\gamma=0}}{T_w - T_i - x(\partial T_B/\partial x)}. \tag{D5}$$

Résumé—Cet article donne les résultats d'une étude théorique et expérimentale de la transmission de chaleur dissymétrique dans le cas d'un écoulement d'air turbulent pleinement établi entre deux plaques lisses parallèles. Les flux de chaleur sur la surface des plaques ayant des valeurs différentes; dans l'étude théorique, on a supposé que les deux flux de chaleur des surfaces étaient uniformes dans la direction de l'écoulement. Dans le travail expérimental, l'écoulement bi-dimensionnel a été réalisé au moyen de conduits à grand allongement.

On a enregistré la distribution des vitesses et le coefficient de frottement de l'écoulement adiabatique et ces résultats sont en bon accord avec ceux que donnent les relations adoptées.

Les mesures d'échange thermique ont été faites d'abord avec une paroi isolée puis avec échange par les deux parois. Dans la dernière série d'expériences, les flux des parois étaient inégaux et de signes contraires. On a observé que la valeur expérimentale du coefficient d'échange thermique, pour la paroi cédant de la chaleur au fluide, est inférieure à la valeur admise dans le cas d'un échange thermique symétrique et qu'elle décroît lorsque le degré de dissymétrie augmente. On a mesuré une diminution du coefficient d'échange allant jusqu'à 40%.

La théorie fondée sur l'analogie entre les transports de chaleur et de quantité de mouvement est plus rigoureuse que celle publiée par l'auteur dans un article précédent et tout à fait bien verifiéé par les données expérimentales.

En conclusion, le coefficient d'échange thermique dépend de la distribution du flux de chaleur sur la périphérie de la section d'écoulement.

Zusammenfassung—Die Ergebnisse einer theoretischen und experimentellen Untersuchung über asymmetrischen Wärmeübergang an Luft bei voll ausgebildeter turbulenter Strömung zwischen zwei ebenen parallelen Platten werden hier angegeben. Der Wärmefluss an den Plattenoberflächen konnte verschiedene Grössen annehmen; für die theoretische Analyse wurde der Wärmefluss an jeder Platte als einheitlich in Strömungsrichtung vorausgesetzt. Die zweidimensionale Strömung liess sich bei den Versuchen durch lange Kanäle mit grossem Seitenverhältnis erreichen. Die aufgezeichneten Werte für die Geschwindigkeitsverteilung und die Reibung in adiabater Strömung zeigten gute Übereinstimmung mit den gemachten Annahmen. Die Messungen für den Wärmeübergang wurden erst für den Fall durchgeführt, dass eine Wand isoliert ist, dann für den Wärmeübergang an beide Wände. Bei letzteren Versuchen war der Wärmefluss beider Platten ungleich und von entgegengesetztem Vorzeichen. Der durch das Experiment ermittelte Wärmeübergangskoeffizient zwischen Wand und Flüssigkeit war kleiner als der angenommene Wert für den Fall des symmetrischen Wärmeübergangs und er nahm ab mit zunehmender Asymmetrie. Diese Abnahme des Wärmeübergangskoeffizienten betrug bis zu 40%.

Die auf der Analogie zwischen Wärme- und Impulsaustausch beruhende Theorie erwies sich zutreffender als die vom Autor in einer früheren Arbeit veröffentlichte und wird von den Versuchsergebnissen gleichermassen gestützt.

Der Wärmeübergangskoeffizient scheint von der Wärmeflussverteilung am Umfang des Strömungsquerschnitts abzuhängen.

Аннотация—В статье представлены результаты теоретического и экспериментального изучения несимметричного теплообмена полностью развившегося турбулентного течения воздуха с ограждающими его двумя гладкими параллельными пластинами. Плотности теплового потока на обеих поверхностях пластин задавались различными по величине. При теоретическом же рассмотрении задачи плотность теплового потока на каждой поверхности принималась одинаковой вдоль по течению среды. Во время экспериментов плоское течение воспроизводилось при помощи длинных каналов с большим относительным удлинением.

Полученные распределения скорости течения и поверхностного трения в адиабатических условиях находятся в хорошем согласии с теоретическими соотношениями. Измерения теплообмена производились для случаев, когда одна из стенок была изолирована, а также при наличии теплообмена на обоих стенках. В последнем случае плотности потоков тепла на стенке были неодинаковы и имели противоположный знак.

Наблюдения показали, что величина экспериментально найденного коэффициента теплообмена для стенки, через которую передавалось тепло движущейся среде, ниже, чем величина, принятая для случая симметричного подвода тепла к пластинам, и что она уменьшается с возрастанием степени асимметрии. Полученное уменьшение коэффициента теплообмена составляет примерно 40% сравнительно со случаем симметричного теплоподвода.

Теория, основанная на аналогии между переносом тепла и количества движения, является более строгой, чем опубликованная автором в предыдущей статье, и достоверно подтверждается полученными экспериментальными данными.

Сделан вывод, что коэффициент теплообмена зависит от распределения плотности теплового потока на ограждающих течение стенках канала.